# Bleaching With Alternative Layered Minerals: A Comparison With Acid-Activated Montmorillonite for Bleaching Soybean Oil[1]

**Dennis R. Taylor, Dennis B. Jenkins** and **Charles B. Ungermann**
Engelhard Corp., P.O. Box 877, Pleasanton, CA 94566

**An extensive series of layered minerals including montmorillonite was studied to determine if the fundamental physicochemical properties responsible for pigment adsorption could be identified. Samples were subjected to a uniform preparation regimen to eliminate such secondary effects as particle size, moisture content, level of activation and degree of washing. By doing so, it has been possible to show that both carotene and chlorophyll adsorptions can be described by a rather simple model that employs both surface acidity and pore volume as key variables. Further, it was found that this model provides an adequate fit to the actual data only when specific regions for these variables are considered (i.e., concentration of sites of strong surface acidity, not just total surface acidity; pore volume in region 50–200 Å, not just total pore volume).**

Acid-activated montmorillonite bleaching clay is the industry standard for removing various trace constituents (chlorophyll, carotenoids, phospholipids, metals and oxidation products) from edible and inedible oils by adsorption. While its pre-eminence in this application has remained unchallenged since its introduction at the beginning of this century (1), it is also fair to say that a complete understanding of the reasons for its dominance (over other clay minerals) is still lacking. This is true in spite of numerous studies (2–8) relating the role of various physical/chemical properties of acid-activated clays to their pigment adsorption efficiencies.

In the present study, we address these issues as part of an on-going effort on our part to more fully ascertain and quantify fundamental properties of surface active minerals as they relate to the adsorption phenomenon. Our approach has been to assemble an extensive set of layered minerals exhibiting both similarities to and differences from montmorillonite, and then to subject the entire set to rigorous chemical/physical characterization and performance testing. Our objective was to identify the key parameters responsible for adsorption by a process of comparative analysis. In order to maximize the study's utility while keeping its scope within reasonable bounds, we examined both nonactivated and acid-activated forms of the study minerals, but restricted the set almost exclusively to the 2:1 class of layered minerals. Some new (synthetic and/or modified) minerals whose bleaching properties have not been described previously have been included for completeness.

Properties of bleaching clays which previously have been ascribed a role in the adsorption of trace constituents from oils include: surface acidity (2,3,6,8), surface area and porosity (3–8), degree of acid activation (2–4,7), particle size (2–4,8), and moisture content (2,5). The criteria we established for choosing study materials involved selecting various layered minerals which were known or expected to possess some degree of surface area, porosity and surface acidity (after acid activation).

Basically, three chemical classes of 2:1 layered minerals (Table 1) are represented in this study: aluminosilicates, magnesium silicates and zirconium phosphates. Aluminosilicates (2:1) and magnesium silicates (2:1) are composed of two (tetrahedrally coordinated) sheets of silica atoms sandwiched about a central (octahedrally coordinated) sheet of either alumina, or magnesia atoms, respectively. The 2:1 zirconium phosphates are composed of two (tetrahedrally coordinated) sheets of phosphate atoms sandwiched about a central (octahedrally coordinated) sheet of zirconate atoms. Stacked (repeating) sheets of these 2:1 layered structures form individual mineral crystallites (in sizes ranging from 0.1 μm up to 2 μm equivalent diameters depending on the specific mineral). Only one of the study minerals, HY-zeolite, does not possess a layered structure: it has a rigid, highly ordered three-dimensional array of structural aluminate and silicate tetrahedra which form a series of connecting pores and chambers containing mobile (exchangeable) cations (9).

TABLE 1

**Study Minerals**

| Name | Code | Source[a] | Chemical type | Layer type |
|---|---|---|---|---|
| HY-Zeolite | HYZ | E | | 3 Dimens |
| Ca-Montmorillonite[b] | CaM | E | | |
| Na-Montmorillonite[c] | NaM | AC | | |
| Low Si/Al ratio SMM[d] | LOSM | E | Alumino- | |
| High Si/Al ratio SMM[d] | HISM | E | silicate | |
| Fe SMM[d] | FeSM | E | | |
| Ni SMM[d] | NiSM | E | | 2:1 |
| Pillared montmorillonite | PILM | E | | |
| Illite | ILL | CMS | | |
| α-$Zr(HPO_4)_2$ (crystalline) | AXZP | E | | |
| α-$Zr(HPO_4)_2$ (pseudocrystalline) | AZP | E | Zirconium phosphate | |
| γ-$Zr(HPO_4)_2$ | GZP | E | | |
| γ-$Zr(HPO_4)_2$ (phenyl pillared) | GPZP | E | | |
| Hectorite[e] | HEC | NL | | |
| Synthetic Hectorite[f] | SHEC | L | Magnesium | |
| Vermiculite | VER | AV | silicate | |
| Chlorite | CHL | W | | 2:1 + 1 |

[a] AC, American Colloid, Skokie, Illinois; CMS, Clay Minerals Society, Bloomington, Indiana; NL, NL Industries, Heightstown, New Jersey; L, Laporte Industries Ltd., Saddle Brook, New Jersey; AV, American Vermiculite, Atlanta, Georgia; W, Wards Natural Science Establishment, Rochester, New York; E, Engelhard, Menlo Park, New Jersey.

[b] Filtrol Gr 160™.

[c] American Colloid Volclay™.

[d] SMM, synthetic mica montmorillonite.

[e] NL Industries Macaloid™.

[f] Laporte Laponite™.

[1] Presented at the AOCS meeting in New Orleans, LA in May 1987.

It was included in the present study because it provided a good control as a nonlayered material which nevertheless possesses high surface area, porosity and surface acidity. In addition, it provides a good comparison for another study material, pillared montmorillonite, which is claimed (Vaughan, D.E.W., and R.J. Lussier, paper presented at the 5th International Conference on Zeolites, Naples, Italy, June 1980) (10) to become "pseudozeolitic" in character once pillared. All of the remaining minerals have a 2:1 layered structure although chlorite contains an extra brucite (MgO) sheet in the interlayer region and therefore possesses a 2:1 + 1 arrangement.

Two other common 2:1 layer aluminosilicates, pyrophyllite and mica, were excluded from the present study because of their low surface areas and known resistance to acid attack (11,12). Likewise kaolin, a well-known 1:1 layer clay mineral composed of one (tetrahedrally coordinated) sheet of silica atoms bonded to a (octahedrally coordinated) sheet of alumina atoms was not included because it does not respond to acid activation. And finally attapulgite, a fibrous clay mineral, was not included because it did not possess the simple layered structure being studied here; bleaching properties for both these latter minerals have been described elsewhere (1,5,8).

## MATERIALS AND METHODS

*Clay activations.* Because maximum clay bleaching efficiency depends in a nonpredictable way on the amount of acid used for activation (2-4,7), each clay sample was subjected individually to an optimization procedure designed to develop the maximum activity achievable for that particular sample. To obtain the optimum acid activated product, a series of screening reactions was performed using activation time as the independent variable. A quantity of each material was reacted at a fixed acid dosage where acid dosage = (g 98% $H_2SO_4$/g clay, ignited basis) × 100% and small samples of slurry were removed at various time intervals. These samples were rinsed, filtered and dried at 35°C in a forced air oven. They were then tested for carotene (carotenoids) and chlorophyll (pheophytins) adsorption efficiency in refined soy oil. Conditions giving the highest adsorption efficiencies were considered optimum and were repeated when preparing larger samples (125-200 g). Several materials were resistant to acid treatment and showed no maxima. For these materials, the maximum activation time (5 hr) was used. As with the screening samples, the final samples were slurried in an acid/water mixture (20 wt% solids) and activated by heating to 100°C using a constantly-stirred glass reaction vessel. A condenser was used to prevent water loss during the activation.

Table 2 gives optimum activation conditions; for most, 200% acid dosage and 100°C were used. The natural and synthetic hectorites reacted (leached) so vigorously that activation time could not be used as the screening variable. Instead, these two materials were screened using a fixed time interval and a variable acid dosage. For these materials the slurry concentration was 10 wt% solids. The layered zirconium phosphates were not activated because they possess a naturally acidic surface (13). Strong acid treatment will collapse pillared montmorillonite, so this material was activated by a very brief (1 min) sulfuric acid treatment to pH 3.3. HY-zeolite was prepared by calcining $NH_4$-Y zeolite at 425°C for 3 hr.

TABLE 2

**Optimum Activation Conditions for Study Minerals**

| Mineral name | Code | Activation conditions: Acid dosage[a] | Time (hr) | Temp. (°C) |
|---|---|---|---|---|
| HY-Zeolite | HYZ | — | 3.0 | 425 |
| Ca-Montmorillonite | CaM | 200% | 1.5 | 100 |
| Na-Montmorillonite | NaM | 200% | 4.3 | 100 |
| Low Si/Al ratio SMM[b] | LOSM | 200% | 0.75 | 100 |
| High Si/Al ratio SMM[b] | HISM | 200% | 0.75 | 100 |
| Fe SMM[b] | FeSM | 200% | 0.42 | 100 |
| Ni SMM[b] | NiSM | 200% | 0.50 | 100 |
| Pillared montmorillonite | PILM | pH 3.3 | 1 min | 25 |
| Illite | ILL | 200% | 4.3 | 100 |
| Hectorite | HEC | 100% | 2.0 | 25 |
| Synthetic hectorite | SHEC | 40% | 2.0 | 25 |
| Vermiculite | VER | 200% | 0.5 | 100 |
| Chlorite | CHL | 200% | 5.0 | 100 |

[a] Acid dosage, (g 98% $H_2SO_4$/g clay, ignited basis) × 100%.
[b] SMM, Synthetic mica montmorillonite.

*General clay preparation.* As mentioned previously, bleaching activity depends on a rather extensive set of factors (2-8). In order to reduce the number of variables, all (acid-activated) samples were subjected uniformly to the following steps: (i) following activation, they were quenched in 12 gallons of DI water to remove excess sulfuric acid, allowed to settle, and the supernatant decanted off; the remaining material was then filtered and rinsed four times with one-l aliquots of deionized water; (ii) the resultant filter cakes were then dried to equilibrium moisture content at 35°C in a forced air oven, and (iii) ground so 100% of the powdered samples would pass through a 200 mesh (75 μm) wire screen sieve.

*Synthetic mica montmorillonites.* Synthetic mica montmorillonite (SMM) and the Fe and Ni substituted forms were prepared by the methods of Granquist (14,15).

*Pillared montmorillonite.* Pillared montmorillonite was prepared by the method of Occelli (16).

*Zirconium phosphates.* Zirconium phosphates were prepared as follows: α-zirconium phosphate (crystalline), method of Alterti and Torracca (17); α-zirconium phosphate (pseudocrystalline), method of Clearfield and Stynes (18); γ-zirconium phosphate, method of Clearfield et al. (19); the phenyl-pillared derivative, method of Yamanaka (20).

*Other minerals.* The other minerals were obtained as follows: sodium montmorillonite (Volclay™), American Colloid, Skokie, Illinois; illite, Clay Minerals Society, Bloomington, Indiana; hectorite (Macaloid™), NL Industries, Heightstown, New Jersey; synthetic hectorite (Laponite™), Laporte Industries Ltd., Saddle Brook, New Jersey; vermiculite, American Vermiculite, Atlanta, Georgia, and chlorite, Wards Natural Science Establishment, Rochester, New York.

*Adsorption efficiency data.* Adsorption efficiencies were determined by contacting the study materials with refined soy oil for 15 min under vacuum (1.5 in. Hg) at 105°C. Residual carotene (carotenoids) and chlorophyll

(pheophytins) contents were measured on the McCloskey Colorimeter (model 01-0120) using a 5.25" cell. Phosphorous data were obtained nephelometrically using the Hach Ratio Turbidimeter (model 18900) (21) and colorimetrically according to the method of Yuen (22). Subtracting these data from the contents of the original oil yields the adsorption data (reported as ppm or ppb/g of clay, dry basis).

*Physicochemical analyses.* Physical and chemical properties of the study minerals were determined as follows: chemical analysis, samples dried at 1000°C and then analyzed for Si, Al, Fe, Ca, Mg, Na, K and Ti using X-ray fluorescence (XRF); Zr and P by ICP; Li by atomic adsorption, and F by ion selective electrode. Slurry pH was measured on an aqueous slurry containing 10% dry material. Surface acidity was determined by the method described by Kladnig (23). Surface area and pore volume were determined on the Quantasorb Sorption system (Quantachrome Corp.) using the BET method with $N_2$ as an adsorbate. Pore volume distribution vs pore diameter was determined using the Digisorb 2500 surface area/pore volume analyzer (Micromeritics). Pore volumes were measured ($N_2$ adsorption and desorption cycles) in six different pore diameter regions (30–50 Å, 50–100 Å, 100–200 Å, 200–300 Å, 300–400 Å, and 400–600 Å). Cation exchange capacity was determined by exchange with strontium ion, followed by XRF chemical analysis for strontium.

## RESULTS AND DISCUSSION

While it is clearly beyond the scope of this study to discuss the structural aspects of these minerals in any detail, it is appropriate to at least highlight their major differences. The archetype, Ca-montmorillonite, is a 2:1 aluminosilicate whose basic structure has already been described *(vide supra).* In addition, some exchangeable calcium ions are present between the layers; further information concerning structural and chemical aspects of montmorillonites is available in two recent reviews (3,4).

When this structure is subjected to acid leaching, removal of structural ions occurs primarily in the central (octahedral) layer (24,25) with two major consequences: (i) the structure is opened up considerably as evidenced by significant increases in surface area (3,4) and porosity (3,4), and (ii) the original interlayer cations (calcium, sodium, potassium) are exchanged with aluminum (as well as some magnesium and ferric) cations which have been freed from the central layer by the leaching process. Because these particular cations are considerably more acidic than the calcium ions they replace, the overall acidity of the leached structure increases as well (26,27). As will be described below, these changes constitute major positive benefits of the acid-leaching process.

The other 2:1 aluminosilicates have basically the same structure as the Ca-montmorillonite, but differ in detail. Pillared montmorillonite, for instance, is prepared by exchanging the original interlayer cations with large (aluminum oxyhydroxide) polycations (28). Because these cations are so large, and because the montmorillonite structure exhibits a capacity for expansion, the distance (d-spacing) between layers is increased from the normal 15 Å up to 18 Å when these ions are inserted between the layers. It is claimed (10) that these altered clays become "pseudozeolitic" in character once they have been pillared.

Synthetic mica-montmorillonite (SMM) used to make (LOSM, HISM, FeSM and NiSM) bleaching clays differs from naturally occurring montmorillonite by virtue of its extreme purity (all ingredients are controlled during synthesis). SMM itself contains only aluminum atoms in its octahedral layer; substitutions by iron or nickel into this layer are made possible by adding these ions to the synthesis mix and give Fe- and Ni-SMM, respectively.

Illite, a naturally occurring mineral closely related to mica, possesses a structure quite similar to the SMM just described. It differs by virtue of possessing a higher degree of negative layer charge (hence much stronger electrostatic attraction between the negative layer charge and the interlayer cations) with the result that the layers are pulled closer together (the d-spacing is typically only about 10 Å for this clay).

Zirconium phosphates represent a new class of synthetic layered minerals that have no naturally occurring analogs. They make excellent additions to the present study because they possess some features similar to montmorillonite (i.e., high surface acidity, moderate-to-good porosity), as well as some substantial differences (i.e., reverse orientation of structural tetrahedra, the presence of structural OH groups in the interlayer region, and the absence of layer charge).

Zirconium phosphates exhibit two different morphologies. The $\alpha$-form is characterized by hydrogen bonding between the apical, interlayers OH groups and the structural zirconate ions in an adjacent layer. This structure possesses a rather low d-spacing of only 7.6 Å. The $\gamma$-form is characterized by hydrogen bonding between the adjacent apical OH groups themselves (between one layer and the next) and possesses a considerably larger d-spacing of about 12.4 Å. As with montmorillonite, these structures can also be "pillared." A phenyl pillared derivative has been included in this study, and possess a d-spacing of about 15.2 Å.

The structure of the magnesium silicates differs from the aluminosilicates by virtue of having all octahedral positions occupied by magnesium ions in the central layer. For both natural and synthetic hectorite, layer charge arises as a consequence of substitution by lithium for magnesium ions in the octahedral layer, whereas for vermiculite, it arises because of substitution by aluminum ions for silicon ions in the tetrahedral layer. Chlorite, a 2:1 + 1 magnesium silicate layer mineral, possess a completely "locked" structure because the interlayer region is occupied by a layer of brucite (MgO). As a consequence, it has no cation exchange capacity.

As shown (Figs. 1-3), surface acidity, surface area and pore volume all increase upon acid activation (the only exception being the pillared montmorillonite which is affected relatively little). Generalizations beyond these, however, are difficult to make. Some of the minerals display large changes in a given parameter upon activation, while others are relatively less affected. For example, sodium montmorillonite (NaM) exhibits a substantial increase in surface acidity (Fig. 1) upon activation, but vermiculite (VER) and chlorite (CHL) increase only moderately. In another example, the surface area (Fig. 2) for vermiculite is substantially increased; in contrast, chlorite increases about one-half, and sodium montmorillonite

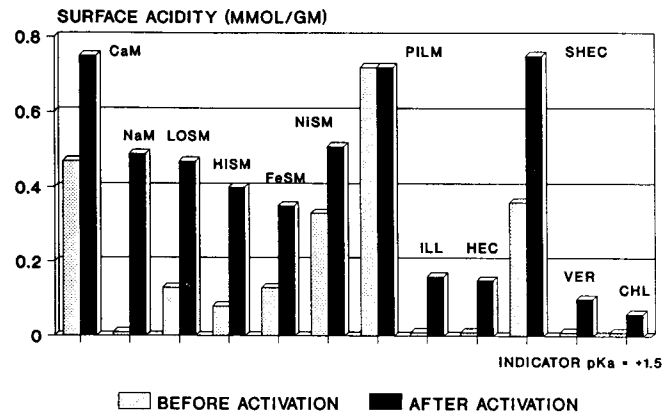


FIG. 1. Activation effect influence on surface acidity.

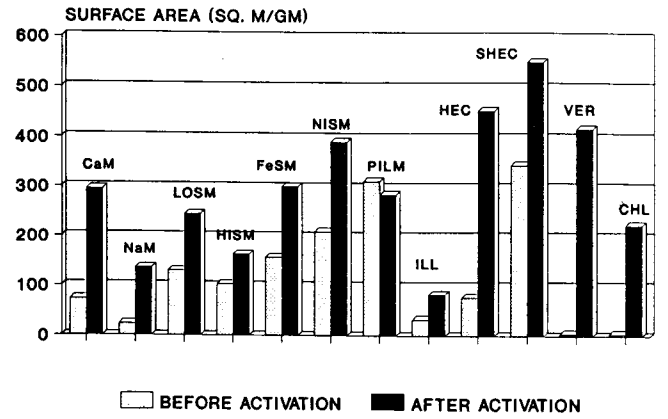


FIG. 2. Activation effect influence on surface area.

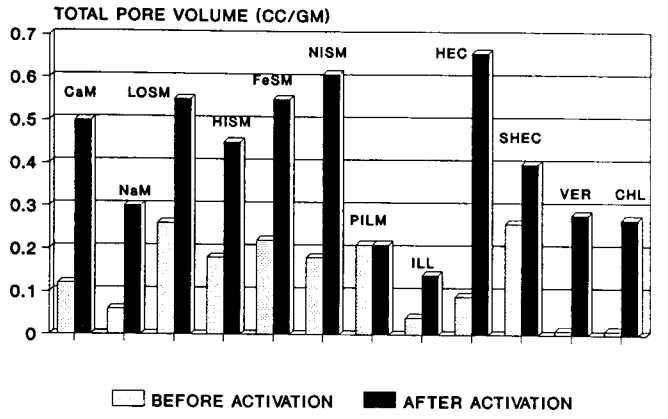


FIG. 3. Activation effect influence on pore volume.

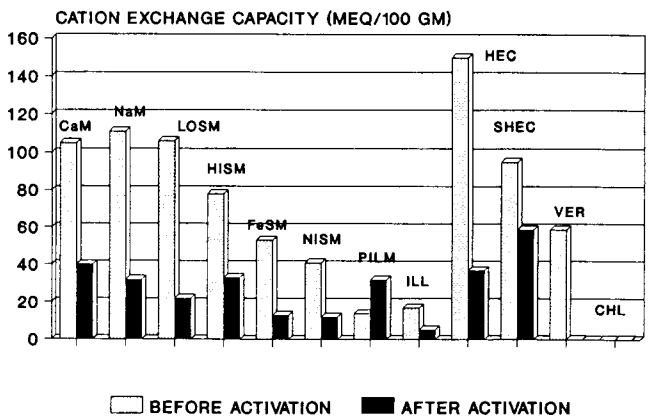


FIG. 4. Activation effect influence on cation exchange capacity.

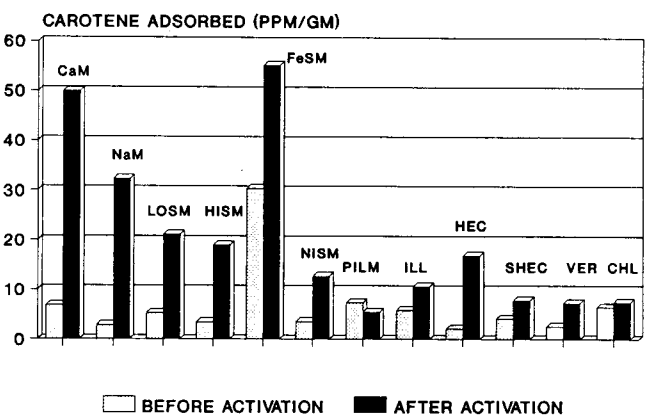


FIG. 5. Activation effect. Carotene adsorption: refined soy oil.

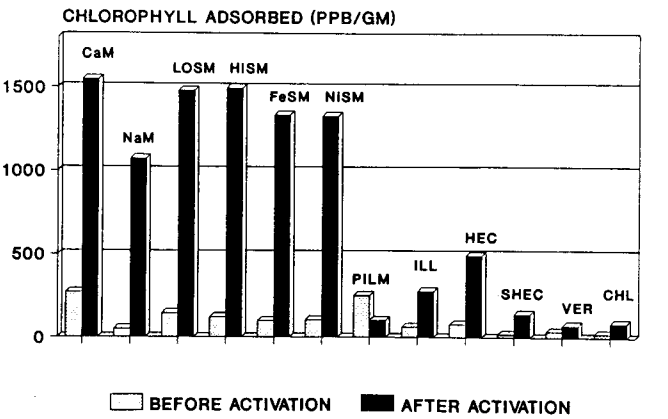


FIG. 6. Activation effect. Chlorophyll adsorption: refined soy.

only about one-third as much. Other examples of non-uniformity in degree of response to acid-activation can be found upon examination of the data in Figure 1-4.

The only study parameter which decreases upon acid activation is cation exchange capacity. The explanation is that the acid-activation process removes structural ions from the octahedral layer (25,26). Their removal, and the simultaneous protonation of the lattice, reduces the need for counterbalancing cations in the interlayer region. Because cation exchange capacity (Fig. 4) is a measure of these interlayer cations, its decrease is to be expected.

Tables 3 and 4 summarize the results obtained when these minerals were used to adsorb various trace constituents from caustic refined and water degummed soybean oils, respectively. These data (represented as bar graphs in Figs. 5-7) attest to the general superiority of acid-

TABLE 3

**Adsorptive Properties of Study Materials**

| Study materials | Contacts w/ refined soybean oil[a] | | | | |
|---|---|---|---|---|---|
| | Chlorophyll[b] (ppb) | LvR[c] | Carotene[d] (ppm) | Adsorbed ch[e] | Adsorbed ca[f] |
| No treatment | 710 | 18.7 | 31 | 0 | 0 |
| HYZ act | 686 | 18.3 | 28 | 63 | 7 |
| CaM raw | 598 | 16.2 | 28 | 272 | 7 |
| act | 78 | 10.7 | 10 | 1548 | 50 |
| NaM raw | 688 | 16.6 | 30 | 52 | 3 |
| act | 245 | 13.5 | 17 | 1073 | 33 |
| LOSM raw | 646 | 16.3 | 29 | 146 | 5 |
| act | 80 | 17.5 | 22 | 1482 | 21 |
| HISM raw | 657 | 16.6 | 29 | 123 | 4 |
| act | 56 | 18.6 | 23 | 1497 | 19 |
| FeSM raw | 668 | 13.7 | 18 | 100 | 30 |
| act | 126 | 8.8 | 7 | 1338 | 55 |
| NiSM raw | 665 | 17.2 | 29 | 105 | 4 |
| act | 132 | 19.4 | 25 | 1330 | 13 |
| PILM raw | 610 | 17.2 | 28 | 253 | 7 |
| act | 668 | 17.1 | 28 | 103 | 5 |
| ILL raw | 682 | 16.5 | 28 | 63 | 6 |
| act | 586 | 17.5 | 26 | 279 | 11 |
| AXZP | 713 | 16.2 | 29 | 0 | 4 |
| AZP | 691 | 18.1 | 27 | 45 | 9 |
| GZP | 681 | 18.1 | 27 | 74 | 9 |
| GPZP | 703 | 19.9 | 27 | 17 | 9 |
| HEC raw | 676 | 16.8 | 30 | 79 | 2 |
| act | 500 | 14.5 | 24 | 493 | 17 |
| SHEC raw | 702 | 16.4 | 29 | 19 | 4 |
| act | 658 | 15.9 | 28 | 140 | 8 |
| VER raw | 694 | 17.5 | 30 | 38 | 3 |
| act | 679 | 16.8 | 28 | 73 | 7 |
| CHL raw | 700 | 17.2 | 28 | 22 | 7 |
| act | 672 | 17.3 | 28 | 86 | 8 |

[a]Contacts with 0.3 wt% dosage in 150 g oil; 220°F for 15 min/28.5″ vac.
[b]Chlorophyll level after contact, ppb.
[c]Lovibond red value after contact.
[d]Carotene level after contact, ppm.
[e]Chlorophyll adsorbed, ppb/g (dry basis).
[f]Carotene adsorbed, ppm/g (dry basis).

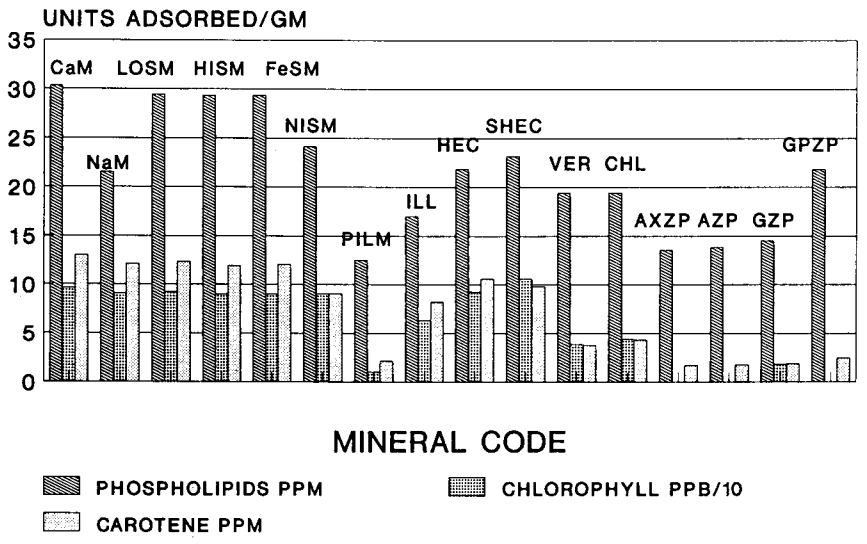


**FIG. 7. Adsorption trace constituents. Activated minerals: soybean oils.**

TABLE 4

**Adsorptive Properties of Study Materials**

| Study materials | | Contacts w/ degummed soybean oil[a] | | | | | | |
|---|---|---|---|---|---|---|---|---|
| | | Phos[b] (ppm) | Chlor[c] (ppb) | LvR[d] | Carot[e] (ppm) | Adsorbed phos[f] | Adsorbed ch[g] | Adsorbed ca[h] |
| No treatment | | 120 | 270 | 20 | 37 | | | |
| HYZ | act | na | na | na | na | | | |
| CaM | raw | | | | | | | |
| | act | 35 | 0 | 1.1 | 0.4 | 30.4 | 96.4 | 13.1 |
| NaM | raw | | | | | | | |
| | act | 56 | 0 | 3.7 | 0.9 | 21.5 | 90.6 | 12.1 |
| LOSM | raw | | | | | | | |
| | act | 34 | 0 | 2.9 | 0.9 | 29.5 | 92.5 | 12.4 |
| HISM | raw | | | | | | | |
| | act | 32 | 0 | 3.3 | 1.2 | 29.3 | 90.0 | 11.9 |
| FeSM | raw | | | | | | | |
| | act | 32 | 0 | 3.4 | 0.8 | 29.3 | 90.0 | 12.1 |
| NiSM | raw | | | | | | | |
| | act | 48 | 0 | 9.2 | 10 | 24.2 | 90.6 | 9.1 |
| PILM | raw | | | | | | | |
| | act | 85 | 242 | 20 | 31 | 12.5 | 10.0 | 2.1 |
| ILL | raw | | | | | | | |
| | act | 68 | 76 | 15.4 | 12 | 17.0 | 63.6 | 8.2 |
| AXZP | | 80 | 273 | 20 | 32 | 13.7 | 0 | 1.7 |
| AZP | | 80 | 273 | 20 | 32 | 13.9 | 0 | 1.7 |
| GZP | | 81 | 221 | 20 | 32 | 14.3 | 17.9 | 1.8 |
| GPZP | | 58 | 283 | 20 | 30 | 21.5 | 0 | 2.4 |
| HEC | raw | | | | | | | |
| | act | 56 | 0 | 8.5 | 6 | 21.9 | 92.5 | 10.6 |
| SHEC | raw | | | | | | | |
| | act | 61 | 0 | 10.9 | 12 | 23.1 | 105.9 | 9.8 |
| VER | raw | | | | | | | |
| | act | 63 | 158 | 20 | 26 | 19.5 | 38.2 | 3.8 |
| CHL | raw | | | | | | | |
| | act | 61 | 137 | 20 | 24 | 19.5 | 43.9 | 4.3 |

[a] Atmospheric contacts, 3 wt% dosage in 100 g oil; 248°F for 15 min.

[b] Phosphorus level, after contact, ppm.

[c] Chlorophyll level after contact, ppb.

[d] Lovibond red value after contact.

[e] Carotene level after contact, ppm.

[f] Phosphorus adsorbed, ppm/g (dry basis).

[g] Chlorophyll adsorbed, ppb/g (dry basis).

[h] Carotene adsorbed, ppm/g (dry basis).

activated montmorillonites vs other layered minerals for this application. And although the acid-activation process obviously enhances the adsorptivity of almost all the study minerals (pillared montmorillonite being the only exception), it is also clear that the response of the montmorillonites to acid activation is significantly greater than that of the other clay minerals (Figs. 5,6).

Of the new materials examined here, only Fe-SMM proved itself to be in a class with Ca-montmorillonite for the adsorption of all three trace constituents after acid-activation (Figs. 5–7). The remaining SMM materials were somewhat better than Na-montmorillonite for adsorption of phospholipids and chlorophyll, but inferior with regard to carotene adsorption. Phospholipids appear to be quite easily adsorbed regardless of the adsorbent being utilized, but the zirconium phosphate materials, in particular, seem to exhibit a truly marked selectivity for this constituent relative to the other layered minerals studied. Although Y-zeolite has been reported (29) to be a relatively poor adsorbent for carotene, pillared (pseudozeolitic) montmorillonite had not been mentioned previously for this application. As with Y-zeolite, however, it proves to be much less efficient than acid-activated montmorillonite for the adsorption of carotenoids and pheophytins. It seems likely that restricted porosity in the 50–200 Å region is responsible for the poor efficiency of both these adsorbents *(vide infra)*.

In searching for a relationship between adsorption and the physical/chemical properties of these minerals, we compared carotene, chlorophyll and phospholipid adsorption vs surface acidity, surface area and pore volume. Because Ni-SMM and Fe-SMM were too highly colored to obtain accurate surface acidity values at pKa = −3, they could not be included in this analysis; also α-zirconium phosphate (crystalline) and phenyl pillared γ-zirconium phosphate were left out because their carotene and chlorophyll adsorption efficiencies were essentially zero. CEC was eliminated as a study variable in this

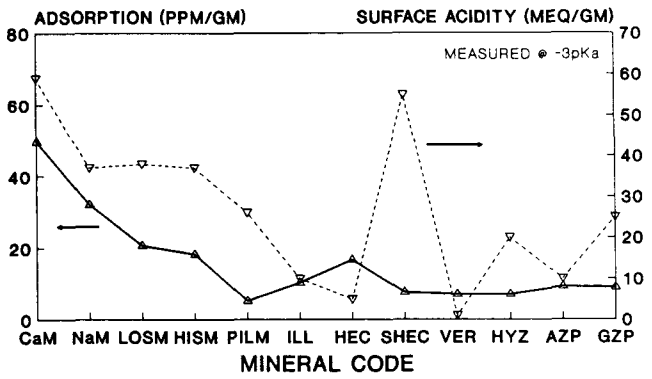


FIG. 8. Carotene adsorption vs surface acidity: refined soy oil.

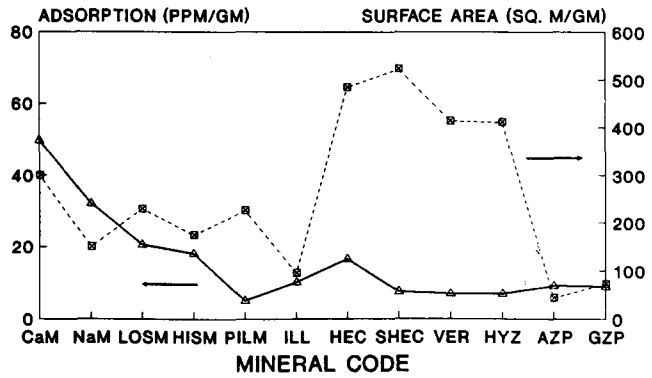


FIG. 9. Carotene adsorption vs surface area: refined soy oil.

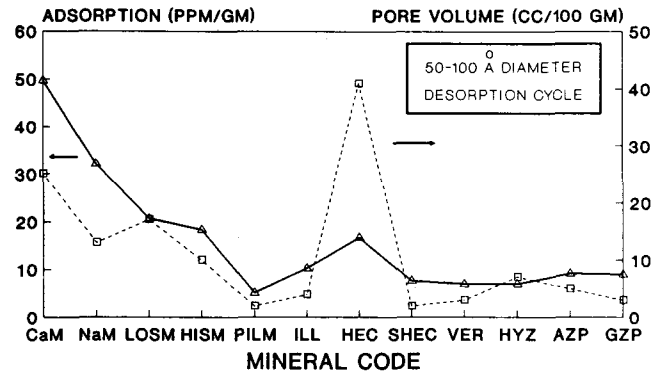


FIG. 10. Carotene adsorption vs pore volume: refined soy oil.

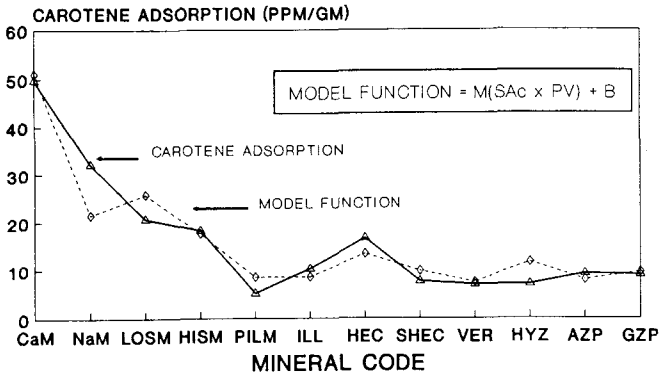


FIG. 11. Carotene adsorption vs model function: refined soy oil.

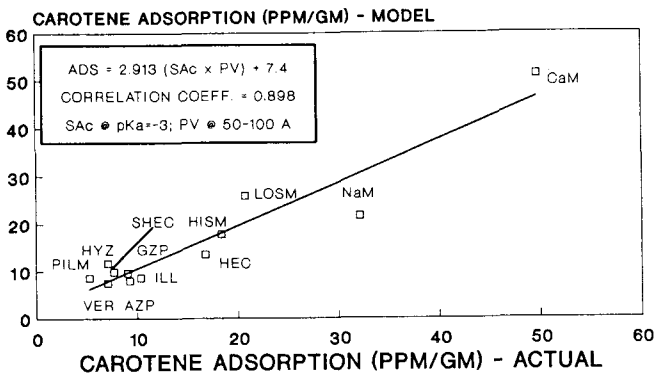


FIG. 12. Carotene adsorption. Actual vs model function.

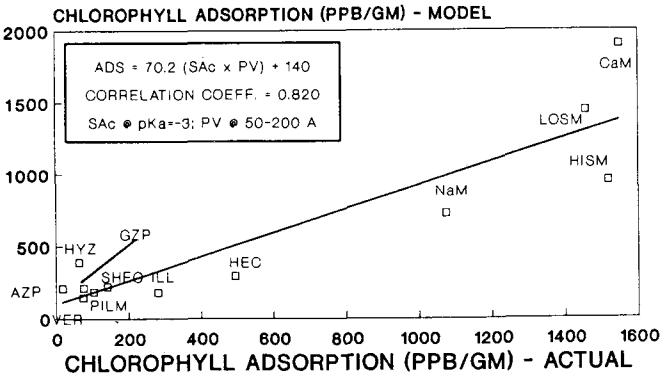


FIG. 13. Chlorophyll adsorption. Actual vs model function.

analysis because of its close relationship to surface acidity. Surface acidity has the added advantage of giving the distribution of site strengths; acidities were measured at pKa = +5, +1.5, −3.

Representative comparisons (Figs. 8-10) did not indicate a significant correlation between adsorption and any single physicochemical property (e.g., there were no close matches between the pattern for pigment adsorption vs mineral type and the corresponding patterns for surface acidity, surface area or pore volume vs mineral type). This situation has been noted previously (3,6,8). Nevertheless, a large body of chemical literature would argue that pigment adsorption should be related in some manner to at least some of these parameters. Of course, adsorption could be related to combinations of these parameters. Working from this premise, we derived a large number of empirical mathematical models using these parameters in various linear and power combinations, and examined their correlation with the actual adsorption data. Utilizing this approach, it has been possible to obtain a linear expression of a model function of the form M(SAc × PV) + B, where SAc = surface acidity, PV = pore volume, and B is an adsorption constant, which correlates reasonably well with the adsorption data for both carotenoids (Fig. 11) and chlorophyll (not shown). When a least squares analysis of the model vs carotene and chlorophyll adsorption data was performed for selected sets of acid-activated minerals (Figs. 12-13), correlation

coefficients of 0.898 and 0.820 were obtained, respectively. The model just described did not provide an adequate fit to the phospholipid adsorption data. As noted above, most zirconium phosphates seem to exhibit an additional (or alternate) mode of interaction with phospholipids that rules out the use of this model for predicting phospholipid adsorption. Based on our analysis, we were unable to conclude that total surface area, *per se,* was a significant determinant as regards carotene and chlorophyll adsorption.

It is to be appreciated, of course, that the pore volume and surface acidity determinations which provided the best fits to the adsorption data depend on the accuracy of the analytical techniques used to obtain them. Pore volume determinations were made on a Micromeritics Digisorb 2500 surface area/pore volume analyzer, an instrumental technique of proven accuracy and reproducibility. Surface acidities, however, were determined by titrations utilizing Hammett indicators, a technique (24) that is not absolute and rather difficult to perform. Nevertheless, on a relative basis, we found the best correlations were obtained when only the strongest acid sites (i.e., $pKa < -3$) were considered. Because both the carotenoids (30) and the pheophytins (31) are weak bases, this kind of dependency seems reasonable if the adsorption phenomenon is a result of an acid-base type interaction (3,6, 8,22). Also noteworthy is the finding that the best correlation regarding carotene adsorption was obtained when using pore volumes in the 50–100 Å pore diameter region ($N_2$ desorption cycle) while for chlorophyll adsorption it was obtained when using pore volumes in the 50–200 Å pore diameter region. Because these pore diameters are considerably larger than the cross sectional dimensions of the corresponding monomeric molecules (*ca.* $7 \times 31$ Å for carotene; $12 \times 15$ Å for chlorophyll) this finding may lend credence to the suggestion of Brimberg (32) that these pigments act as colloids dispersed in the oil (or that they are in a colloidal state when they interact with adsorbent clays).

The implications of the model just described are that the best adsorbents will be those which have, simultaneously, a high concentration of strong acid sites and high pore volumes concentrated in pores whose diameters fall in the 50–200 Å region. On the basis of this model, we can rationalize the poor performance of various members of the study set. Hectorite, for instance, possesses a very high pore volume in the 50–100 Å region (Fig. 10) but, unfortunately, one of the lowest surface acidities (Fig. 8). Synthetic hectorite, possessing the reverse characteristics (low pore volume but high surface acidity), is also a relatively poor adsorbent in this application. Even differences between samples of the same mineral species such as Ca- vs Na-montmorillonite can be explained on the basis of this model: Ca-montmorillonite, after activation, possesses the highest levels of both surface acidity and porosity (in the desired region) of any of the minerals studied. The Na-montmorillonite used here, even though chemically almost indistinguishable from the Ca-analog after activation, nevertheless ends up possessing somewhat lower surface acidity and porosity characteristics. Consequently, it is a less active adsorbent for carotenoids and chlorophyll.

Because the model described above successfully fits the data for a broad range of (layered) mineral types which possess significant variability in their physicochemical signatures, we believe the model has general validity. Finally, utilizing this model, we can begin to understand why certain acid-activated clay minerals (Ca-montmorillonites, in particular) are superior to other clay minerals in this application (i.e., they possess high levels of both strong acid sites and pore volume in the 50–200 Å region after activation). Additional work is under way in our laboratory to refine and further test the conclusions of this study.

## REFERENCES

1. Rich, A.D., in *Industrial Minerals and Rocks,* 3rd edn., American Institute of Mechanical Engineers, New York, NY, 1960, pp. 93–101.
2. Richardson, L.L., *J. Am. Oil Chem. Soc. 55*:777 (1978).
3. Taylor, D.R., and D.B. Jenkins, *Society of Mining Engineering of the American Institute of Mechanical Engineers, Tras. 282*:1901 (1988).
4. Fahn, R., *Acid-Activated Clays and Their Adsorption Properties,* SME reprint 79-328, SME-AIME Fall Meeting, Tucson, Arizona, Oct. 1979, 13 pp.
5. Khoo, L.E., F. Morsingh and K.Y. Liew, *J. Am. Oil Chem. Soc. 56*:672 (1979).
6. Liew, K.Y., S.H. Tan, F. Morsingh and L.E. Khoo, *Ibid. 59*:480 (1982).
7. Kheok, S.C., and E.E. Lim, *Ibid. 59*:129 (1982).
8. Morgan, D.A., D.B. Shaw, M.J. Sidebottom, J.C. Soon and R.S. Taylor, *Ibid. 62*:292 (1985).
9. Breck, D.W., *Zeolite Molecular Sieves,* John Wiley & Sons, New York, NY, 1973, pp. 92–104.
10. Shabtai, J., R. Lazar and A.G. Oblad, *Proc. 7th Inter. Congress Catalysis,* edited by T. Seiyama and K. Tanabe, Kodansha-Elsevier, Tokyo, 1980, pp. 828–837.
11. Rodriquez, J.L., C. Maqueda and A. Justo, *Clays Clay Miner. 33*:563 (1985).
12. Reynolds, R.C., and P. Lessing, *Am. Mineral. 47*:979 (1962).
13. Clearfield, A., and D.S. Thakur, *Applied Catalysis 26*:1 (1986).
14. Granquist, W., G. Hoffman and R. Boteler, *Clays Clay Miner. 20*:323 (1972).
15. U.S. Patent 3,852,405 (1974).
16. Occelli, M.L., and R.M. Tindwa, *Clays Clay Miner. 31*:22 (1983).
17. Alterti, G., and E. Torracca, *J. Inorg. Nucl. Chem. 30*:318 (1968).
18. Clearfield, A., and J.A. Stynes, *Ibid. 26*:117 (1964).
19. Clearfield, A., R.H. Blessing and J.A. Stynes, *Ibid. 30*:2249 (1968).
20. Yamanaka, S., and M. Hattori, *Inorg. Chem. 20*:1929 (1981).
21. Sinram, R.D., *J. Am. Oil Chem. Soc. 63*667 (1986).
22. Yuen, W.K., and P.C. Kelly, *Ibid. 57*:339 (1980).
23. Kladnig, W., *J. Phys. Chem. 80*:262 (1976).
24. Osthaus, B., *Clays Clay Miner. 4*:301 (1956).
25. Carroll, D., and H. Starkey, *Ibid. 19*:321 (1971).
26. Mortland, M., and K. Raman, *Ibid. 16*:393 (1968).
27. Frenkel, M., *Ibid. 22*:435 (1974).
28. Lahav, N., U. Shani and J. Shabtai, *Ibid. 26*:107 (1978).
29. Liew, K.Y., F. Morsingh, S.H. Tan and L.E. Khoo, *Palm Oil Technology—80's,* Paper T12, Research Institute of Malaysia, Kuala Lumpur, 1980.
30. Deno, M., H.B. Richey, J.D. Hodge and M.J. Wisotsky, *J. Am. Chem. Soc. 84*:1498 (1962).
31. Delaporte, N., D. Laval-Martin, *Analusis 1*:289 (1972).
32. Brimberg, U.I., *J. Am. Oil Chem. Soc. 59*:74 (1982).

[Received May 10, 1988;
accepted October 21,1988]